A Potential for a Three-Field AdS/QCD Model

Sean P. Bartz*and Joseph I. Kapusta†

January 14, 2014

Abstract

The Anti-de Sitter Space/Conformal Field Theory (AdS/CFT) correspondence may offer new and useful insights into the non-perturbative regime of strongly coupled gauge theories such as Quantum Chromodynamics (QCD). We present an AdS/CFT-inspired model that describes the spectra of light mesons. The conformal symmetry is broken by a background dilaton field, and chiral symmetry breaking and linear confinement are described by a chiral condensate field. These background fields, along with a background glueball condensate field, are derived from a potential. We describe the construction of the potential, and the calculation of the meson spectra, which match experimental data well. We also argue that the presence of the third background field is necessary to properly describe the meson spectra. The outlook for application of this model to finite temperature systems is also discussed.

*E-mail: bartz@physics.umn.edu
†E-mail:kapusta@physics.umn.edu

1 Introduction

The Anti-de Sitter Space/Conformal Field Theory (AdS/CFT) correspondence is a useful mathematical tool for the analysis of strongly-coupled gauge theories. This correspondence correspondence establishes a connection between an n-dimensional Super-Yang Mills Theory and a weakly-coupled gravitational theory in $n+1$ dimensions. Calculations that are analytically intractable in the field theory can be related to results from the gravity theory using an effective dictionary developed over the past decade. Quantum chromodynamics (QCD) is a strongly-coupled gauge theory at hadronic scales, making it a candidate for the application of the gauge/gravity correspondence. It is not known whether a gravitational dual to QCD exists, but there has been much work on models that capture its key features. The bottom-up approach assumes the existence of such a dual, modeling features of QCD by an effective five-dimensional gravity theory. Linear confinement in QCD sets a scale that is encoded in a cut-off of the fifth dimension in the AdS/QCD model. So-called soft-wall models use a dilaton field as an effective cut-off to limit the penetration of the meson fields into the bulk. The simplest soft-wall models use a quadratic dilaton to recover the linear Regge trajectories, while models that modify the UV behavior of the dilaton more accurately model the ground state masses.

The soft-wall models typically include at least two background fields: the aforementioned dilaton, and a chiral condensate field that corresponds to the chiral symmetry breaking in the gauge theory. These models use parametrizations for the background dilaton and chiral fields that are not derived as the solution to any equations of motion. A well-defined action would provide a set of background equations from which these fields can be derived, and may suggest how the model can be derived from a top-down approach. In addition, this action provides access to the thermal properties of the model through perturbation of the geometry.

In this paper, we expand upon previous attempts to find a suitable potential for the background fields of a soft-wall AdS/QCD model. After demonstrating the limitations of models including a dilaton and chiral field alone, we suggest the inclusion of a background glueball field. We then construct a potential that satisfies the necessary UV and IR limits, and use this potential to generate numerically the background fields and calculate the resulting meson spectra.

2 Review and Motivation

Previous work showed how to construct a potential for a gravity-dilaton-chiral system, assuming that the fields have power-law behavior, which is accurate in both the UV and IR limits. One of the equations of motion is independent of the choice of potential,

$$\dot{\chi}^2 = \frac{\sqrt{6}}{z^2}\frac{d}{dz}(z^2\dot{\phi}). \tag{1}$$

Examining the IR limit, we know that the dilaton should have quadratic behavior, $\phi(z) = \lambda z^2$. Inserting this into , we find that the chiral field behaves as

$$\chi(z) = 6^{3/4}\sqrt{\lambda}z, \tag{2}$$

which removes one of the independent parameters of the original GKK model. As shown in that paper, the IR coefficient of the chiral field sets the large-n mass splitting between the axial-vector and vector mesons in the model. Using the phenomenological value of λ, which determines the slope of the Regge trajectories, we find a mass splitting that is much too large.

Because this problem arises in the equation that does not involve the potential, this issue cannot be resolved by the choice of potential in the two-field model. Models that derive the field behavior using the superpotential method suffer from the same problem.

To resolve this problem, we suggest to add an additional scalar field to the model, G, representing the glueball condensate. This field must be linear in the IR for linear confinement, and go as z^4 in the UV to match the operator dimension in the AdS/CFT dictionary.

3 Setup

Consider the action in the string frame for three fields: ϕ, χ and G representing the dilaton, a chiral field, and a glueball field with zero mass

$$S_{string} = \frac{1}{16\pi G_5}\int d^5x\sqrt{-g}e^{-2\Phi}\left(R_s\partial_\mu\Phi\partial^\mu\Phi - \tfrac{1}{2}\partial_\mu\chi\partial^\mu\chi - \tfrac{1}{2}\partial_\mu G\partial^\mu G - e^{-4\Phi/3}V(\phi,\chi,G)\right) \tag{3}$$

The potential in the Einstein frame, where the action has its canonical form, is

$$V(\phi,\chi,G) = \mathrm{e}^{2\phi/\sqrt{6}}\,\tilde{V}(\phi,\chi,G) \tag{4}$$

with

$$\tilde{V} = -12 + 4\sqrt{6}\phi + a_0\phi^2 - \tfrac{3}{2}\chi^2 + \tilde{U} \tag{5}$$

Here $\tilde{U}$ is more than quadratic in the fields. The dilaton mass is undetermined and is not connected to the dimension of the corresponding operator, as discussed by Kapusta and Springer. It is related to the parameter a_0 by $a_0 = \frac{1}{2}\left[(m_\phi L)^2 - 8\right]$. The potential should be an even function of χ.

The equations of motion can be written as

$$\dot{\chi}^2 + \dot{G}^2 = \frac{\sqrt{6}}{z^2}\frac{d}{dz}(z^2\dot{\phi}) \tag{6}$$

$$\tilde{U} = \tfrac{1}{2}\sqrt{6}z^2\ddot{\phi} - \tfrac{3}{2}(z\dot{\phi})^2 - 3\sqrt{6}z\dot{\phi} - 4\sqrt{6}\phi - a_0\phi^2 + \tfrac{3}{2}\chi^2 \tag{7}$$

$$\frac{\partial\tilde{U}}{\partial\phi} = 3z\dot{\phi} - 2a_0\phi \tag{8}$$

$$\frac{\partial \tilde{U}}{\partial \chi} = z^2 \ddot{\chi} - 3z\dot{\chi}\left(1 + \frac{z\dot{\phi}}{\sqrt{6}}\right) + 3\chi \tag{9}$$

$$\frac{\partial \tilde{U}}{\partial G} = z^2 \ddot{G} - 3z\dot{G}\left(1 + \frac{z\dot{\phi}}{\sqrt{6}}\right) \tag{10}$$

We assume that the potential has no explicit dependence on the coordinate z, so the equations 8-10 are not independent, and we can eliminate one.

3.1 IR Limit

The requirement of linear confinement requires a solution in the large z limit of the form

$$\phi = \lambda z^2 \tag{11}$$

$$\chi = Az \tag{12}$$

$$G = Bz. \tag{13}$$

Substitution into (6) gives

$$A^2 + B^2 = 6\sqrt{6}\lambda \tag{14}$$

The λ is fixed by the slope of the linear trajectory and A is fixed by the axial-vector – vector mass difference. It is useful to write these as

$$A = 6^{3/4}\sqrt{\lambda}\cos\theta$$

$$B = 6^{3/4}\sqrt{\lambda}\sin\theta, \tag{15}$$

where θ now becomes the parameter controlling the axial-vector – vector mass splitting. Inserting (13) into (7-10) suggests the following terms in our ansatz for the potential

$$\tilde{U} = a_1\phi\chi^2 + a_2\phi G^2 + a_3\chi^4 + a_4 G^4 + a_5\chi^2 G^2 + a_6 G^2\tanh(g\phi). \tag{16}$$

We see that there must be a G^2 term in the IR limit, but this is forbidden in the weak-field limit because the glueball condensate field is massless. To circumvent this, we propose the term $G^2\tanh(g\phi)$ with $g > 0$. In the weak field limit this goes to $g\phi G^2$, which is acceptable. The tanh is suggested by (4), and it suggests a rapid exponential transition from the weak field to the strong field limits that is supported by phenomenology. By substitution one finds the following constraints on the parameters:

$$\tilde{U} \to 6 + a_0 + 6\sqrt{6}\left(\cos^2\theta\, a_1 + \sin^2\theta\, a_2\right)$$

$$+6^3\left(\cos^4\theta\, a_3 + \sin^4\theta\, a_4 + \cos^2\theta\sin^2\theta\, a_5\right) = 0 \tag{17}$$

$$\frac{\partial \tilde{U}}{\partial \chi} \to 2a_1 + 24\sqrt{6}\cos^2\theta\, a_3 + 12\sqrt{6}\sin^2\theta\, a_5 + \sqrt{6} = 0 \tag{18}$$

$$\frac{\partial \tilde{U}}{\partial G} \to 2a_2 + 24\sqrt{6}\sin^2\theta\, a_4 + 12\sqrt{6}\cos^2\theta\, a_5 + \sqrt{6} = 0 \tag{19}$$

$$\frac{\partial \tilde{U}}{\partial G} \to a_6 = -\tfrac{3}{2} \tag{20}$$

We have chosen to exclude (8) because it is not independent. The parameter a_6 is determined, and the others will be determined by an examination of the UV limit.

3.2 UV Limit

Next we look for a solution in the small z limit. The AdS/CFT dictionary dictates that the leading-order UV behavior of the chiral and glueball condensate fields is determined by their dimension. Note also that we are working in the chiral limit where the quark mass is zero. We start by examining only the leading-order terms

$$\chi = \Sigma_0 z^3 \tag{21}$$

$$G = G_0 z^4. \tag{22}$$

Substitution into (6) and imposing the boundary condition $\phi(0) = 0$ gives

$$\phi = \frac{\sqrt{6}}{28}\Sigma_0^2 z^6 + \frac{\sqrt{6}}{27}G_0^2 z^8 \tag{23}$$

Using only this leading-order behavior in (7-10), the system of equations is inconsistent, as there are more equations from matching powers of z than unknown parameters.

To solve this problem, try adding a term $\Sigma_n z^n$ to χ. Substituting into (6) and keeping only the lowest-order cross-term we find the additional term in ϕ

$$\Delta\phi = \frac{\sqrt{6}n\Sigma_0\Sigma_n}{(n+4)(n+3)} z^{n+3} \tag{24}$$

From (7) we find that

$$\tilde{U} = -\tfrac{3}{2}(z\dot{\phi})^2 - a_0\phi^2 + 3\frac{n^3 - 13n + 12}{(n+4)(n+3)}\Sigma_0\Sigma_n z^{n+3} \tag{25}$$

Since the ϕ^2 terms start out as z^{12}, z^{14}, z^{16}, and so do the terms in the potential, the n can only take the values 9, 11, etc. This term contributes only to the equation for $\partial\tilde{U}/\partial\chi$.

$$\frac{\partial \tilde{U}}{\partial \chi} = -9\Sigma_0\left(\frac{3}{14}\Sigma_0^2 + \frac{8}{27}G_0^2 z^2\right) z^9 + (n-3)(n-1)\Sigma_n z^n \tag{26}$$

By power counting both $n = 9$ and $n = 11$ can contribute.

There could also be higher order terms in G such as $G_m z^m$. This leads to the additional term in ϕ

$$\Delta\phi = \frac{8mG_0G_m}{\sqrt{6}(m+5)(m+4)} z^{m+4} \tag{27}$$

It contributes to the equation for $\partial\tilde{U}/\partial G$ as

$$\frac{\partial\tilde{U}}{\partial G} = -12G_0\left(\frac{3}{14}\Sigma_0^2 + \frac{8}{27}G_0^2z^2\right)z^{10} + m(m-4)G_n z^m \tag{28}$$

The choice $m = 8$ is not possible as there is no term of the same order to balance it. Terms with $m = 10$ and $m = 12$ are possible. These new terms cannot affect the equation for $\partial\tilde{U}/\partial\phi$ nor can they contribute to the equation for $\partial\tilde{U}/\partial\chi$. Considering higher order terms in both χ and G leads to

$$\tilde{U} = -\tfrac{3}{2}(z\dot{\phi})^2 - a_0\phi^2 + 3\frac{n^3-13n+12}{(n+4)(n+3)}\Sigma_0\Sigma_n z^{n+3} + \frac{4m(m-4)}{m+4}G_0G_m z^{m+4} \tag{29}$$

The appearance of these terms can be understood by writing the following schematic expansions.

$$\chi \sim \Sigma_0 z^3 + \Sigma_0^3 z^9 + G_0^2\Sigma_0 z^{11} + \cdots$$

$$G \sim G_0 z^4 + \Sigma_0^2 G_0 z^{10} + G_0^3 z^{12} + \cdots$$

That is, χ is an odd function of Σ_0 and G is an odd function of G_0. These are the symmetries in the equations of motion. They also follow the spirit of the AdS/CFT correspondence in terms of the dimensionality of the operators and the powers of z.

Including now $m = 10$ and 12, and $n = 9$ and 11, we have the following set of equations in the small z limit:

$$\begin{aligned}
\tilde{U}_{\rm LHS} &= 3\Sigma_0^4 z^{12}\left[4\frac{\Sigma_9}{\Sigma_0^3} - \frac{(54+a_0)}{2^3\cdot 7^2}\right] \\
&+ \frac{1}{7}\Sigma_0^2G_0^2z^{14}\left[120\frac{G_{10}}{\Sigma_0^2G_0} + 120\frac{\Sigma_{11}}{\Sigma_0G_0^2} - \frac{(72+a_0)}{9}\right] \\
&+ 2G_0^4z^{16}\left[12\frac{G_{12}}{G_0^3} - \frac{(96+a_0)}{3^5}\right]
\end{aligned} \tag{30}$$

$$\begin{aligned}
\tilde{U}_{\rm RHS} &= \Sigma_0^4 z^{12}\left[\frac{\sqrt{6}}{28}a_1 + a_3\right] \\
&+ \Sigma_0^2G_0^2z^{14}\left[\frac{\sqrt{6}}{27}a_1 + \frac{\sqrt{6}}{28}(a_2+ga_6) + a_5\right] \\
&+ G_0^4z^{16}\left[\frac{\sqrt{6}}{27}(a_2+ga_6) + a_4\right]
\end{aligned} \tag{31}$$

$$\left(\frac{\partial\tilde{U}}{\partial\chi}\right)_{\rm LHS} = 3\Sigma_0^3 z^9\left[-\frac{9}{14}+16\frac{\Sigma_9}{\Sigma_0^3}\right]+8\Sigma_0 G_0^2 z^{11}\left[-\frac{1}{3}+10\frac{\Sigma_{11}}{\Sigma_0 G_0^2}\right] \quad (32)$$

$$\left(\frac{\partial\tilde{U}}{\partial\chi}\right)_{\rm RHS} = \Sigma_0^3 z^9\left[\frac{\sqrt{6}}{14}a_1+4a_3\right]+\Sigma_0 G_0^2 z^{11}\left[\frac{2\sqrt{6}}{27}a_1+2a_5\right] \quad (33)$$

$$(34)$$

$$\left(\frac{\partial\tilde{U}}{\partial G}\right)_{\rm LHS} = 6\Sigma_0^2 G_0 z^{10}\left[-\frac{3}{7}+10\frac{G_{10}}{\Sigma_0^2 G_0}\right]+32 G_0^3 z^{12}\left[-\frac{1}{9}+3\frac{G_{12}}{G_0^3}\right] \quad (35)$$

$$\left(\frac{\partial\tilde{U}}{\partial G}\right)_{\rm RHS} = \Sigma_0^2 G_0 z^{10}\left[\frac{\sqrt{6}}{14}(a_2+ga_6)+2a_5\right]+G_0^3 z^{12}\left[\frac{2\sqrt{6}}{27}(a_2+ga_6)+4a_4\right] \quad (36)$$

Altogether, from both the UV and IR limits, there are ten independent equations for the twelve parameters $a_0 - a_6$, Σ_9, Σ_{11}, G_{10}, G_{12}, and g. We take g as the free parameter to use as the rate of transition from small z to large z. The parameters in the potential are found to be

$$a_0 = \frac{3}{2}\frac{1}{6+\sin^2\theta}\left[120+62\sin^2\theta+63\sqrt{6}g\sin^2\theta\right] \quad (37)$$

$$a_1 = -\frac{3\sqrt{6}}{4}\frac{1}{6+\sin^2\theta}\left[12+8\sin^2\theta+9\sqrt{6}g\sin^2\theta\right] \quad (38)$$

$$a_2 = -\frac{\sqrt{6}}{4}\frac{1}{6+\sin^2\theta}\left[32+24\sin^2\theta+3\sqrt{6}g(9\sin^2\theta-2)\right] \quad (39)$$

$$2a_3\cos^2\theta+a_5\sin^2\theta = \frac{1}{24}\frac{1}{6+\sin^2\theta}\left[24+22\sin^2\theta+27\sqrt{6}g\sin^2\theta\right] \quad (40)$$

$$2a_4\sin^2\theta+a_5\cos^2\theta = \frac{1}{24}\frac{1}{6+\sin^2\theta}\left[20+22\sin^2\theta+3\sqrt{6}g(9\sin^2\theta-2)\right] \quad (41)$$

$$a_6 = -\frac{3}{2} \quad (42)$$

The coefficients a_0, a_1, a_2 and a_6 are determined, while there are two equations for the three coefficients a_3, a_4 and a_5. That leaves a_5 as a free parameter, to be fit numerically, along with g, θ, G_0, Σ, and λ.

4 Numerical Solution

Using the above potential, we seek a numerical solution that simultaneously satisfies the UV and IR limits. We use equations (6, 9, 10), which allows for an additional term in the potential, $\Delta\tilde{U}$, such that

$$\frac{\partial\Delta\tilde{U}}{\partial\chi} = \frac{\partial\Delta\tilde{U}}{\partial G} = 0, \quad (43)$$

which will be determined from the numerical solution.

The differential equations represent a stiff system, and treatment of the problem as an initial value problem leads to numerical instabilities. We treat it instead as a boundary value problem, using Dirichlet boundary conditions at both boundaries. A relaxation method is used in combination with input approximations for the background fields, which are then iterated to find a stable solution to the system with the given boundary conditions. Because the system is nonlinear, the solution found is not guaranteed to be unique.

The IR boundary is chosen to be sufficiently large to capture the infrared behavior and to give accurate Regge behavior large-n radial excitations of the mesons. The UV boundary should approach zero, but it cannot reach zero because of the singularity in the equations of motion. This becomes a problem because equation (6) allows constant and divergent terms

$$\Delta\phi(z) = c_1 + c_2 z^{-1}. \tag{44}$$

Symbolically, these terms can be set to zero by enforcing the Dirichlet boundary condition $\phi(0) = 0$, but this is impossible to enforce numerically. Creative choice of UV boundary conditions can eliminate one, but not both of these unwanted terms without affecting the chiral and glueball fields. The behavior of the numerical solutions suggests that the desired UV behavior is an unstable solution to the equations, and therefore difficult or impossible to find with this iterative method.

As an alternative to direct solution, we parameterize the fields as follows:

$$\Psi(z) = \psi(z)_{UV} f(z) + \psi(z)_{IR} \left(1 - f(z)\right), \tag{45}$$

where $f(z)$ is some function that transitions smoothly from 1 at small values of z to 0 at large z, and $\psi(z)_{xx}$ represents the known UV and IR limits of the fields ϕ, χ, and G. The switching functions f need not be the same for each field. We choose

$$f_\phi(z) = e^{-(\beta_1 z)^{10}} \tag{46}$$

$$f_\chi(z) = e^{-(\beta_2 z)^{4}} \tag{47}$$

$$f_G(z) = e^{-(\beta_3 z)^{5}}. \tag{48}$$

The powers of the exponential are chosen to be greater than the known power-law behavior of the fields in the UV limit, so as to not interfere with this behavior. The β_i will be set by numerical fitting.

In all, we have nine parameters to be set numerically. The first constraint is to obtain the best global visual fit to the meson spectrum. We do not simply do a chi-squared fitting to the experimental data because the measurement error for the ground state ρ meson is so much smaller than for the others that this would effectively act as the only constraint. Secondly, we seek to minimize the error in the finite-difference approximations to equations 6, 9, and 10.

Three of the parameters are most phenomenologically relevant: λ, which controls the slope of the meson spectra in the large-n limit; θ, which controls

$\lambda^{1/2}$	430 MeV	a_5	25.342
$\Sigma^{1/3}$	210 MeV	β_1	47.42
$G_0^{1/4}$	397 MeV	β_2	0.80
θ	1.44	β_3	0.782
g	1.0		

Table 1: Best fit parameters

α_1	39.26	α_2	52.45
b_1	0.9967	b_2	1.408
c_1	0.5931	c_2	0.7019

Table 2: The parameters for the fitting to $\Delta\tilde{U}$

the mass splitting between the a_1 and ρ mesons, and β_2, which controls the location of the "bend" in the a_1 spectrum. For each set of these parameters, the other parameters are set by a routine that minimizes the error in the equations of motion. The parameters found are shown in Table 1.

We now analyze the "extra" term in the potential, $\Delta\tilde{U}$. This term can be approximated numerically as the sum of two Gaussians of the dilaton,

$$\Delta\tilde{U}(\phi) = \alpha_1 e^{-((\phi-b_1)/c_1)^2} + \alpha_2 e^{-((\phi-b_2)/c_2)^2}. \tag{49}$$

The best-fit values for these parameters are shown in Table 4.

5 Meson Spectra

We use the meson action and equations of motion found in the paper by Gherghetta, Kapusta, and Kelley. This model finds a better phenomenological fit than the results presented in that paper, particularly for the ground state ρ meson. The scalar mesons are expected to mix with the scalar glueball field of this model, and this analysis is not performed here.

Finally, the pion spectrum is analyzed in the same way as in the paper by Kelley, Bartz, and Kapusta. We find similar results, with the exception that the ground state pion is massless in this model, due to the assumption of massless quarks. The transition to the large-n behavior occurs at $n = 3$. It is important to note that the experimental pion data was not used as an input to fit the parameters.

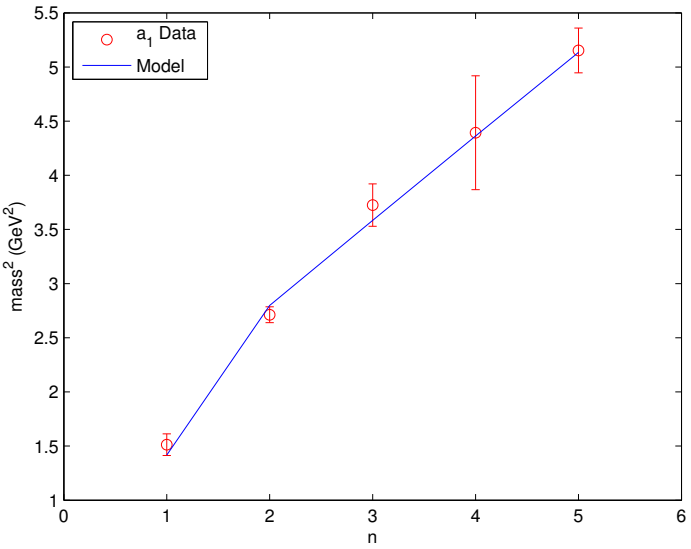

Figure 1: a_1 spectrum.

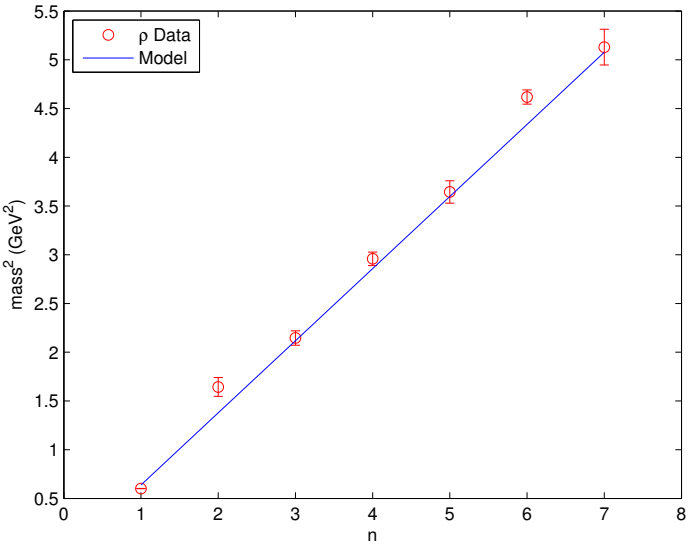

Figure 2: ρ spectrum.

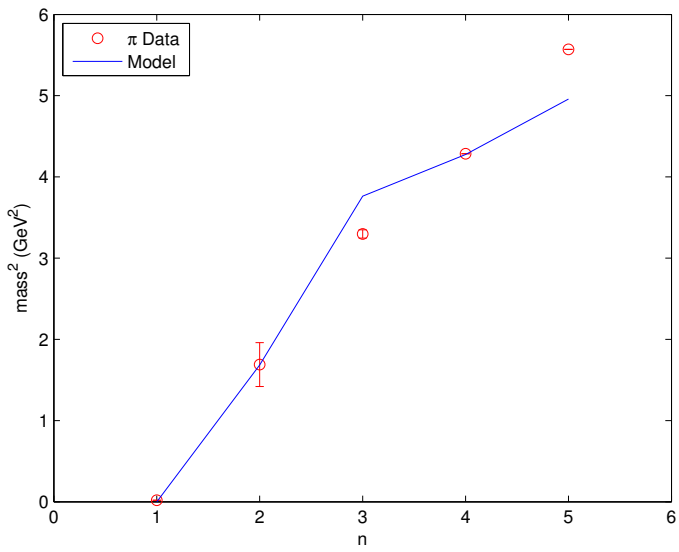

Figure 3: *Pion spectrum. The ground state is massless in the chiral limit. The model was calculated with* $\kappa = 0$ *in the meson action. The* $n = 4, 5$ *states are unconfirmed and are found only in the extended version of the PDG.*